[8] S. Vaez-Zadeh, "Variable flux control of permanent magnet synchronous motor drives for constant torque operation", IEEE Trans. on Pow. Elect., Vol.16, No.4, pp.527-534, July 2001.
[9] S. Vaez, V.I. John, "Minimum loss operation of PM motor drives", IEEE/CCECE. Vol.1, pp.284-287, Montreal, Sep. 1995.
[10] S. Vaez, M.A. Rahman, "Energy saving vector control strategies for electric vehicle motor drives", Conference record of the 1997 IEEE PCC conference, pp.13-18, 1997.
[11] R.E. Fairbain, R.G. Harley, "On-line measurement of synchronous machine parameters", IEEE Trans. Ind. Appl., Vol.28, No.3, pp.639-645, 1992.
[12] L. Salvatore, S. Stasi, "Application of EKF to parameter and state estimation of PMSM drive", IEE Proc.-B, Vol.139, No.3, pp.155-164, 1992.
[13] K.H. Kim, S.K. Chung, G.W.Moon, I.C.Baik, M.J.Youn, "Parameter estimation and control for permanent magnet synchronous motor drive using model reference adaptive technique", IEEE/IECON, Vol.1, pp.387-392, Orlando, 1995.
[14] H. Kim, J. Hartwig, R.D. Lorenz, "Using on-line parameter estimation to improve efficiency of IPM machine drives", IEEE/PSEC, Vol.2, pp.815-820, June 2002.
[15] T. Du, P. Vas, F. Stronach, "Design and application of extended observers for joint state and parameter estimation in high-performance AC drives", Proc. Inst. Elect. Eng.-Elect. Pow. Applicat., Vol.142., No.2, pp.71-78, 1995.
[16] P.H. Millor, "Estimation of parameters and performance of rare earth permanent magnet motors avoiding measurement of load angle", IEE Proc., Part B, Vol.138, pp.322-330, Nov. 1991.
[17] T. Abbasian, "Adaptive control of induction motors with taking core loss into account", Ms. Thesis, Tehran University, Sep. 2005.
[18] K. Khalil Hassan, Nonlinear systems. 2nd ed. Upper addle river, NJ:Prentice-Hall, 1996.
[19] R. Marino, S. Peresada, P. Vagili, "Adaptive input-output linearizing control of induction motors", IEEE Trans. Auto. Cont., Vol.38, No.2, pp.208-221, Feb. 1993.

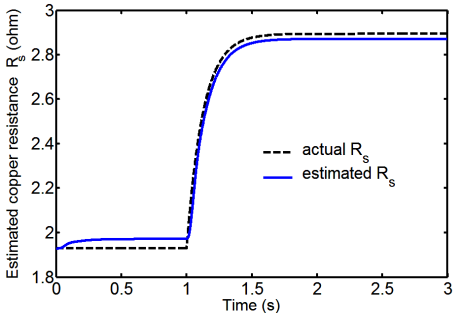

Fig. (17): Actual and estimated R_s

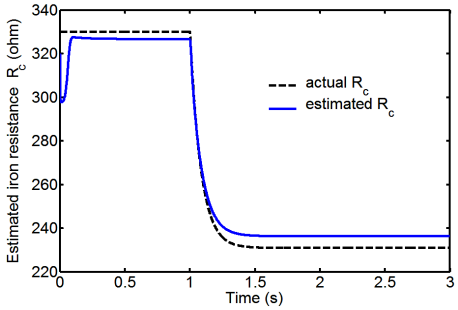

Fig. (18): Actual and estimated R_c

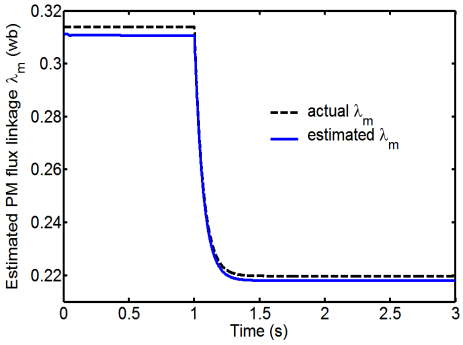

Fig. (19): Actual and estimated λ_m

VII. Conclusion

In this paper, efficiency optimization control of IPM synchronous motors based on input-output feedback linearization was presented. It was shown by extensive analysis and simulation that the variations of motor parameters substantially influence the motor minimum loss condition; resulting in a relatively low motor efficiency even under an efficiency controller. Thus, an accurate, fast and rather simple observer was proposed for the on-line estimation of three motor parameters. In particular the on-line estimation of equivalent iron loss resistance was presented. It was confirmed that the motor parameter estimation can substantially improve the effectiveness of the efficiency optimization control.

Acknowledgement

The support of Center of Excellence on Applied Electromagnetic Systems at the University of Tehran is appreciated.

Appendix I

Machine Specifications

Rated speed,rpm 1800	R_s, R_c Ω	1.93 , 330
Rated torque, Nm 3.96	L_d, L_q mH	42.44 , 79.5
Rated current, A 3	λ_m , Wb	0.314
P, No. of polepairs 2	J, rotor inertia, $Kg.m^2$	0.003
B, Viscous coefficient, Nm / tad / sec. 0.0008		

Appendix II

The coefficients a_0-a_4 of equation (10) are:

$$a_0 = (R_s + R_c)L_d\lambda_m^4\omega_e^2 - \frac{4T_e^2}{9P^2}(L_d - L_q)\left(R_sR_c^2 + (R_s + R_c)L_q^2\omega_e^2\right) \quad (40)$$

$$a_1 = \lambda_m^3\left(R_sR_c^2 + (R_s + R_c)\right)\left(4L_d - 3L_q\right)L_d\omega_e^2\right) \quad (41)$$

$$a_2 = 3(L_d - L_q)\lambda_m^2\left(\frac{R_sR_c^2 + (R_s + R_c)}{(2L_d - L_q)L_d\omega_e^2}\right) \quad (42)$$

$$a_3 = (L_d - L_q)^2\lambda_m\left(\frac{3R_sR_c^2 + (R_s + R_c)}{(4L_d - L_q)L_d\omega_e^2}\right) \quad (43)$$

$$a_4 = (L_d - L_q)^3\left(R_sR_c^2 + (R_s + R_c)L_d^2\omega_e^2\right) \quad (44)$$

References

[1] R. Schiferl, T.A. Lipo, "Power capability of salient pole permanent magnet synchronous motors in variable speed drive application", IEEE Trans. Ind. Appl., Vol.26, No.1, pp.115-123, Jan/Feb. 1990.

[2] K.J. Tseng, S.B. Wee, "Analysis of flux distribution and core losses in interior permanent magnet motor", IEEE Trans. On energy conversion, Vol.14, No.4, Dec. 1999, pp.969-975.

[3] S. Morimoto, Y. Takeda, T. Hirasa, "Loss minimization control of permanent magnet synchronous motors", IEEE Trans. Ind. Elec., Vol.41, pp.511-517, Oct. 1994.

[4] S. Vaez, V.I. John, M.A. Rahman, "An on-line loss minimization controller for interior permanent magnet motor drives", IEEE Trans. on ener. Conv., pp.1435-1440, Dec. 1999.

[5] D. Grenier, L. Dessaint, O. Akhrif, Y. Bonnassieux, B.Le Pioufle, "Experimental nonlinear torque control of a permanent magnet synchronous motor using saliency", IEEE Trans. on indu. Elec., Vol.44, No.5, pp.680-687, Oct. 1997.

[6] C. Mademlis, I. Kioskeridis, N. Margaris, "Optimal efficiency control strategy for interior permanent-magnet synchronous motor drives," IEEE Trans. on energy conversion, Vol.19, No.4, pp.715-723, Dec. 2004.

[7] O. Ojo, F. Osaloni, Z. Wu, M. Omoigui, "A control strategy for optimum efficiency operation of high performance interior permanent magnet motor drives", IEEE/IAS, Vol.1, pp.604-610, Oct. 2003.

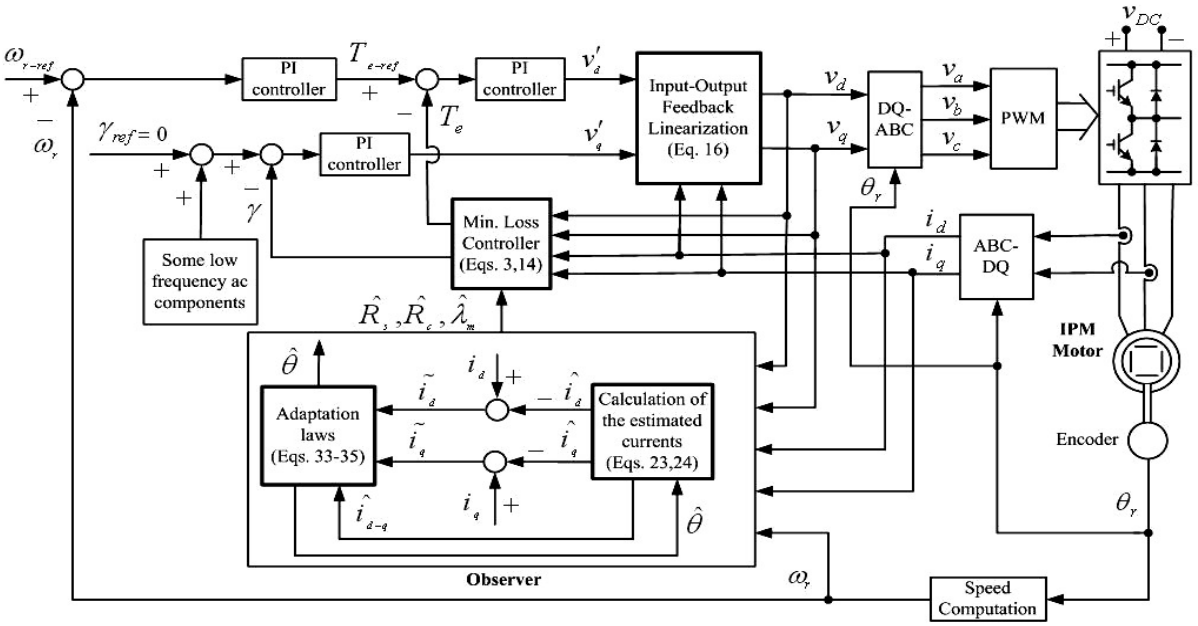

Fig. (12): IPM synchronous motor drive system with input-output feedback linearization, loss minimization controller and observer

The negligible mismatches between the estimated and the actual values of motor parameters seen in Figs 17-19 are not estimation errors associate with the estimation method. They are due to the assumption of $R_c \pm R_s \cong R_c$.

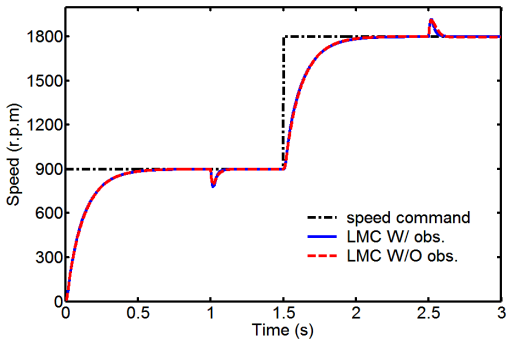

Fig. (13): Speed response

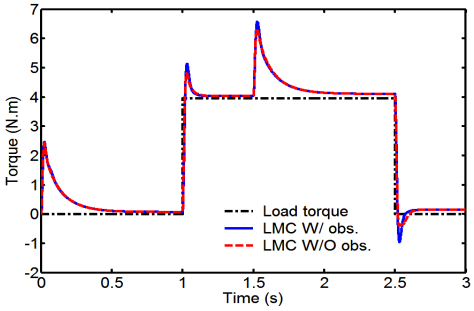

Fig. (14): Torque response

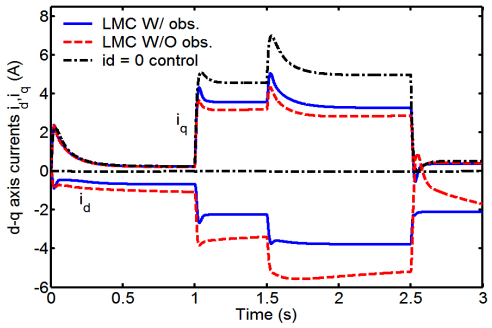

Fig. (15): The d- and q- axis currents

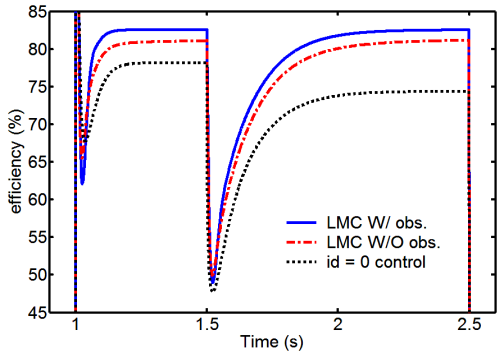

Fig. (16): Motor efficiency

A sinusoidal function with low amplitude and low frequency is added to the reference γ_{ref} in order to satisfy the PE condition. The main parts of the drive system are rather self explanatory as the governing equations are mentioned in each block.

Extensive steady state and dynamic simulation results provided by Matlab Simulink are presented to verify the proposed motor drive control system. Efficiency of the motor with and without observer is shown in Figs. 10-11 for varying speed (at nominal torque) and varying torque (at nominal speed) respectively. It can be seen that parameter variations, without parameter estimation, has undesirable effect on the motor efficiency except in near the nominal operating conditions. This is in agreement with the conclusion drawn in section III. The observer is desirably effective in operating the motor with a higher efficiency over a wide operating range.

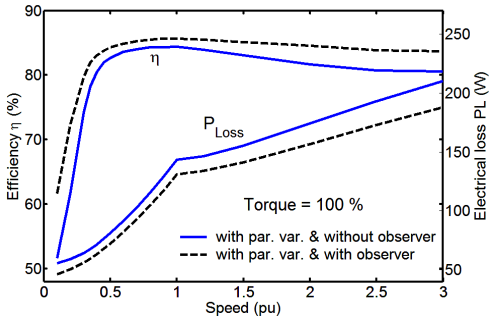

Fig. (10): Motor efficiency versus motor speed with and without observer.

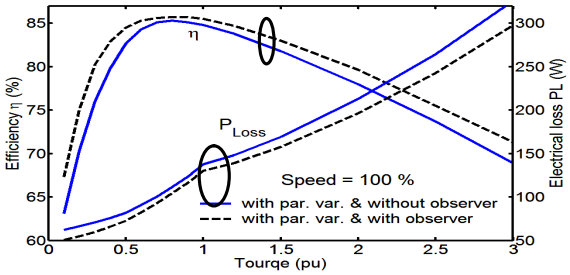

Fig. (11): Motor efficiency versus motor torque with and without observer

Figs. 13-19 show the dynamic performance of the motor drive system. In order to evaluate the controller performance, the motor is started under no load condition in response to a medium size speed command of 900 rpm. At t=1 second the nominal load torque is applied to the motor. Also at t=1.5 second another step speed command is added to the previous command. Finally the load torque is removed at t=2.5 second. The motor speed commands and speed response over this profile can be seen in Fig. 13. Also the load torque and the motor torque are shown in Fig. 14. Figs. 13 and 14 show a fast, accurate and smooth motor operation under the proposed system. The corresponding d- and q-axis currents are also shown in Fig. 15 along with the currents under i_d=0 control and under the loss minimization controller without observer. The plots of motor efficiency during the profile are shown in Fig. 16 for the cases of Fig. 15. The plots show considerable efficiency improvements due to the operation of loss minimization controller and observer. Figs. 17-19 show the estimated values of R_s, R_c and λ_m when their actual values vary. It is assumed that at t=1 second the actual motor copper resistance increases exponentially due to the ambient temperature as seen in Fig. 17. It is seen that the estimated values of R_s follow their actual values quite accurately. It is also assumed that at t=1 second the actual R_c and λ_m reduce exponentially as seen in Figs. 18 and 19 respectively. It is seen that the estimated and the actual values of the latter two motor parameters are in good agreement. The results presented in Figs. 17-19 confirm the effectiveness of the proposed observer in estimating the motor parameters accurately and rapidly.

$$\beta = \frac{1}{R_s + R_c}, \alpha = \beta R_s, \gamma = \beta R_s^2, \sigma = \beta R_s \lambda_m \quad (20)$$

the machine equations are then transformed to:

$$Pi_d = \frac{1}{L_d}(-R_s + \gamma) i_d + \frac{L_q}{L_d}\omega_e i_q + \frac{1}{L_d}(1-\alpha)v_d - \frac{L_q}{L_d}\beta\omega_e v_q + \beta p v_d \quad (21)$$

$$Pi_q = -\frac{L_d}{L_q}\omega_e i_d + \frac{1}{L_q}(-R_s + \gamma) i_q + \frac{L_d}{L_q}\beta\omega_e v_d + \frac{1}{L_q}(1-\alpha)v_q + \frac{1}{L_q}(-\lambda_m + \sigma)\omega_e + \beta p v_q \quad (22)$$

Now an observer is proposed as:

$$p\hat{i}_d = -\frac{1}{L_d}(\hat{R}_s + \hat{\gamma})\hat{i}_d + \frac{L_q}{L_d}\omega_e \hat{i}_q + \frac{1}{L_d}(1-\hat{\alpha})v_d - \frac{L_q}{L_d}\hat{\beta}\omega_e v_q + \hat{\beta} p v_d + f_d \quad (23)$$

$$p\hat{i}_q = -\frac{L_d}{L_q}\omega_e \hat{i}_d + \frac{1}{L_q}(-\hat{R}_s + \hat{\gamma})\hat{i}_q + \frac{L_d}{L_q}\hat{\beta}\omega_e v_d + \frac{1}{L_q}(1-\hat{\alpha})v_q + \frac{1}{L_q}(-\hat{\lambda}_m + \hat{\sigma})\omega_e + \hat{\beta} p v_q + f_q \quad (24)$$

where f_d and f_q are the observer design functions and will be presented later. The estimated quantities are shown as $\hat{x}$. The error dynamics for the proposed observer are obtained by subtraction (23)-(24) from (21)-(22) as:

$$P\tilde{i}_d = -\frac{1}{L_d}(\tilde{R}_s \hat{i}_d + R_s \tilde{i}_d) + \frac{1}{L_d}(\tilde{\gamma}\hat{i}_d + \gamma \tilde{i}_d) + \frac{L_q}{L_d}\omega_e \tilde{i}_q - \frac{v_d}{L_d}\tilde{\alpha} - \frac{L_q}{L_d}\tilde{\beta}\omega_e v_q + \tilde{\beta} p v_d - f_d \quad (25)$$

$$p\tilde{i}_q = -\frac{L_d}{L_q}\omega_e \tilde{i}_d - \frac{1}{L_q}(\tilde{R}_s \hat{i}_q + R_s \tilde{i}_q) + \frac{1}{L_q}(\tilde{\gamma}\hat{i}_q + \gamma \tilde{i}_q) + \frac{L_d}{L_q}\tilde{\beta}\omega_e v_d - \frac{1}{L_q}\tilde{\alpha} v_q + \frac{1}{L_q}(-\tilde{\lambda}_m + \tilde{\sigma})\omega_e + \tilde{\beta} p v_q - f_q \quad (26)$$

where the error quantities are shown as $\tilde{x} = x - \hat{x}$. Now the functions f_d and f_q are presented as:

$$f_d = k_{fd}\tilde{i}_d \ , \ f_q = k_{fq}\tilde{i}_q \quad (27)$$

where k_{fd} and k_{fq} are the constant designed parameters. By substitution (27) into (25)-(26), the latter equations can be rewritten in the matrix form as:

$$pe = A'e + W^T\tilde{\theta} \quad (28)$$

where:

$$e = [\tilde{i}_d \quad \tilde{i}_q]^T \ , \tilde{\theta} = [\tilde{R}_s \quad \tilde{\gamma} \quad \tilde{\alpha} \quad \tilde{\beta} \quad \tilde{\lambda}_m \quad \tilde{\sigma}]^T \quad (29)$$

$$A' = \begin{bmatrix} \frac{-R_s+\gamma}{L_d} - k_{fd} & \frac{L_q}{L_d}\omega_e \\ -\frac{L_d}{L_q}\omega_e & \frac{-R_s+\gamma}{L_q} - k_{fq} \end{bmatrix} \quad (30)$$

$$W^T = \begin{bmatrix} -\frac{\hat{i}_d}{L_d} & \frac{\hat{i}_d}{L_d} & -\frac{v_d}{L_d} & -\frac{L_q}{L_d}\omega_e v_q + p v_d & 0 & 0 \\ -\frac{\hat{i}_q}{L_q} & \frac{\hat{i}_q}{L_q} & \frac{-v_q}{L_q} & \frac{L_d}{L_q}\omega_e v_d + p v_q & -\frac{\omega_e}{L_q} & \frac{\omega_e}{L_q} \end{bmatrix} \quad (31)$$

Now, a Lyapunov function is designed as:

$$V = \frac{1}{2}e^T e + \frac{1}{2}\tilde{\theta}^T \Gamma^{-1}\tilde{\theta} \quad (32)$$

where Γ=diag (k_1, k_2, k_3, k_4, k_5, k_6) and the elements of Γ are constant designed parameters. A time derivative of V, using (28), is given as:

$$pV = e^T A' e + \tilde{\theta}^T W_e + \tilde{\theta}^T \Gamma^{-1} p\tilde{\theta} \quad (33)$$

Assuming the adaptation law as:

$$p\tilde{\theta} = -\Gamma W e \quad (34)$$

then $pV = e^T A' e$. Elements of matrix A' are the parameters to be designed such that A' is a negative

$$p\tilde{\theta} = p\theta - p\hat{\theta} \approx -p\hat{\theta} \quad (35)$$

From (34) and (35) in connection with (28) the adaptation laws in the form of six differential equations are obtained. It is quite time consuming for the control system processor to solve these equations online. Fortunately by using a reasonable approximation as $R_c \pm R_s \cong R_c$, the coefficient of the machine equations (21)-(22) are simplified. This results in a remarkable reduction in the number of adaptation laws to only three equations as the following:

$$p\hat{R}_s = k_1\left\{\left(-\frac{\hat{i}_d}{L_d}\right)\tilde{i}_d + \left(-\frac{\hat{i}_q}{L_q}\right)\tilde{i}_q\right\} \quad (36)$$

definite matrix; then $PV \le 0$. Assume that R_s, R_c and λ_m are unknown constants, then:

$$p\hat{\beta} = k_2\left\{\left(-\frac{L_q}{L_d}\omega_e v_q + p v_d\right)i_d + \left(\frac{L_d}{L_q}\omega_e v_d + p v_q\right)\tilde{i}_q\right\} \quad (37)$$

$$p\hat{\lambda}_m = k_3\left\{-\frac{\omega_e}{L_q}\tilde{i}_q\right\} \quad (38)$$

Now R_s and λ_m are estimated from (37) and (38), respectively, and R_c is estimated as $\hat{R}_c = 1/\hat{\beta}$. Since pV is bounded, it can be claimed that $\tilde{i}_d$, $\tilde{i}_q$ and $\tilde{\theta}$ are bounded. From Barbalat's Lemma it is easy to see that $\lim \tilde{i}_d = 0$, $\lim \tilde{i}_q = 0$ while $t \to \infty$ [18]. This means that the observer error converges to zero if the persistent excitation (PE) condition is satisfied and also the vector θ must converge to zero. The PE condition for this problem implies that there should exist some $\xi > 0$ such that for $t > 0$, the following equation is satisfied:

$$\int_t^{t+\xi} W(\tau)W^T(\tau)d\tau \ge c\, I > 0 \quad (39)$$

where c is any positive value and I is an identity matrix. In order to achieve (39), a low frequency ac component should be added to the reference γ_{ref} [19]. Therefore, if the PE condition is satisfied, the pair (e,θ) globally converges to zero.

VI. Evaluation of Motor Drive Control System

The proposed control and observer algorithms have been applied to an 1hp IPM motor whose data are listed in Appendix I. The drive system block diagram including the input-output feedback linearization, loss minimization controller and the observer is shown in Fig. 12.

$$S_{Rc}=\frac{\partial i_{dT}}{\partial R_c}=-\frac{1}{K}\left(\frac{\partial a_4}{\partial R_c}i_{dT}^4+\frac{\partial a_3}{\partial R_c}i_{dT}^3+\frac{\partial a_2}{\partial R_c}i_{dT}^2+\frac{\partial a_1}{\partial R_c}i_{dT}+\frac{\partial a_0}{\partial R_c}\right) \quad (12)$$

$$S_{\lambda m}=\frac{\partial i_{dT}}{\partial \lambda_m}=-\frac{1}{K}\left(\frac{\partial a_4}{\partial \lambda_m}i_{dT}^4+\frac{\partial a_3}{\partial \lambda_m}i_{dT}^3+\frac{\partial a_2}{\partial \lambda_m}i_{dT}^2+\frac{\partial a_1}{\partial \lambda_m}i_{dT}+\frac{\partial a_0}{\partial \lambda_m}\right) \quad (13)$$

where $K = 4a_4 i_{dT}^3 + 3a_3 i_{dT}^2 + 2a_2 i_{dT} + a_1$ Figs.7-9 show the above sensitivities over a wide range of motor operating conditions. Figs. 7 and 8 imply that the sensitivities of i_{dT} to R_s and R_c in high speeds are significant. The figures also show that the sensitivities are almost independent of motor torque. Fig. 9 shows that the sensitivity of i_{dT} to λ_m is particularly significant at high speed and low torque conditions and, vice versa, at low speed and high torque conditions.

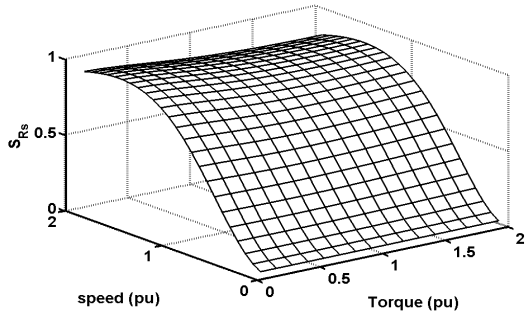

Fig. (7): Sensitivity of optimal i_{dT} to R_s

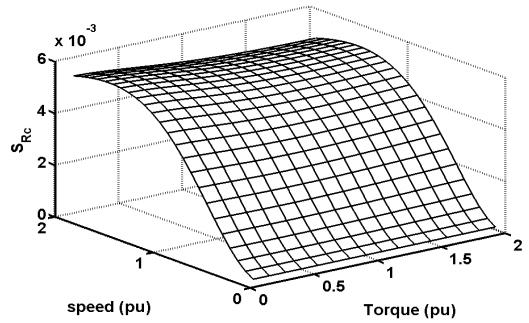

Fig. (8): Sensitivity of optimal i_{dT} to R_c

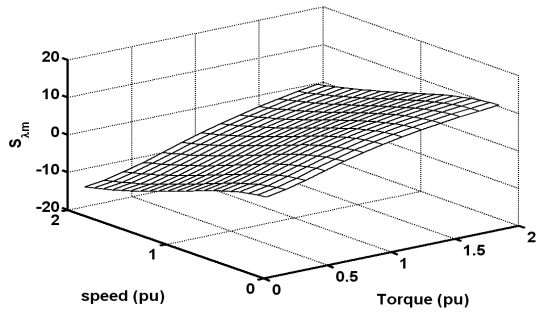

Fig. (9): Sensitivity of optimal i_{dT} to λ_m

A parameter observer will be presented in section V to prevent the energy that could be lost, even under an EOC, due to the high sensitivities shown above.

IV. Efficiency Optimization Controller

The condition for minimum loss operation can be derived by solving (10). However, dynamic solution of such an equation is difficult [3]. In this section another method for achieving minimum loss operation in addition to a high performance control is used [7]. This is done by designing a feedback linearization control in connection with a loss minimization controller as follows.

If γ is defined as:

$$\gamma=\frac{\partial P_L}{\partial i_{qT}}\frac{\partial T_e}{\partial i_{dT}}-\frac{\partial P_L}{\partial i_{dT}}\frac{\partial T_e}{\partial i_{qT}} \quad (14)$$

a minimum total loss for a given torque is then achieved if $\gamma=0$ [7]. In order to reach the control objectives, the motor torque and the function γ are chosen as outputs, i.e. $y_1=T_e$ and $y_2=\gamma$. The input-output linearization technique is then applied to the system (1)-(3) [5]. The outputs y_1 and y_2 have to be successively derived with respect to time, until one of the components of the control vector $u=(v_d \; v_q)^T$ appears.

The system in the matrix form is presented as:

$$P\begin{pmatrix}y_1\\y_2\end{pmatrix}=Au+B \;,\; A=\begin{bmatrix}a_{11} & a_{12}\\ a_{21} & a_{22}\end{bmatrix} \;,\; B=\begin{bmatrix}b_1\\b_2\end{bmatrix} \quad (15)$$

where the components of A and B depend on the machine quantities and parameters. Also A is nonsingular for any feasible operating point.

Indeed, $detA=a_{11}a_{22}-a_{12}a_{21}$ could only reach zero, in the case of the studied motor (see the Appendix I), if i_q >20A, which is not an admissible current value for the motor and the PWM inverter. The input-output linearizing feedback for system (15) is given by [5]:

$$u=\begin{pmatrix}v_d\\v_q\end{pmatrix}=A^{-1}\left(-B+\begin{pmatrix}v'_d\\v'_q\end{pmatrix}\right) \quad (16)$$

where $v=(v'_d,v'_q)^T$ is the new input vector. Substituting (16) into (15) yields:

$$py_1=v'_d \;,\; py_2=v'_q \quad (17)$$

Now a simple PI controller can be designed as:

$$v'_d=py_1=K_{pT}(T_{ref}-T_e)+K_{iT}\int(T_{ref}-T_e)\,dT \quad (18)$$

$$v'_q=py_2=-K_{p\gamma}\gamma-K_{i\gamma}\int\gamma dt \quad (19)$$

where k_{pT}, $k_{p\gamma}$ are the proportional gains and k_{iT}, $k_{i\gamma}$ are the integral gains of the proposed PI controller.

V. Parameter Observer

In this section, a novel observer for the estimation of the stator resistance (R_s), the equivalent iron loss resistance (R_c) and magnetic flux linkage (λ_m) is proposed. The following new parameters are defined to simplify the calculations [17]:

Of course, this value of i_{dT} is not a true optimal i_{dT} when motor parameters vary and results in suboptimal values of P_L corresponding to points A_1, A_2 and A_3. Fortunately, at this nominal operation, the suboptimal values are slightly (up to %3) different from the minimum values of P_L corresponding to B, C and D respectively as mentioned in [3].

Fig. 3 shows the motor electrical loss at a non-nominal motor operation of %50 the nominal torque and %200 the nominal speed. At these operating conditions the differe–nces between the optimal and the suboptimal values of P_L are much larger (up to about %10) than those of Fig. 2. Simultaneous variations of parameters may result in even larger differences between optimal and suboptimal values of P_L. These differences clarify the necessity for on-line parameter estimation in model based EOC of IPM synch–ronous motors in order that the control system is able to find out and apply to the motor a true optimal i_{dT} as a co–mmand signal over a wide range of operating conditions.

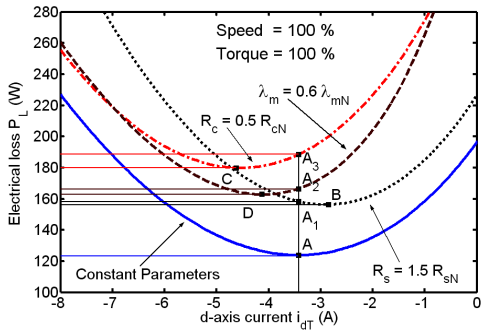

Fig. (2): Influence of parameter variations on minimum P_L at nominal operating conditions

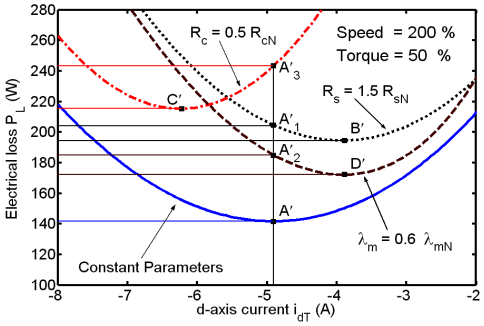

Fig. (3): Influence of parameter variations on minimum P_L at non-nominal operating conditions

Another aspect of the motor parameter variations can be studied by changing the motor parameters over wide ranges and observing its effects on the optimal i_{dT} at different operating conditions. This can be carried out by differentiating the right hand side of (9) with respect to i_{dT} and equating the result to zero to obtain the following eq uation:

$$A_4 i_{dT}^4 + a_3 i_{dT}^3 + a_2 i_{dT}^2 + a_1 i_{dT} + a_0 = 0 \qquad (10)$$

where a_0 – a_4 are given in Appendix II. An optimal value for i_{dT} is achieved by solving (10). Figs. 4-6 show the variations of optimal value of i_{dT} versus R_s, R_c and λ_m respectively at different operating conditions.

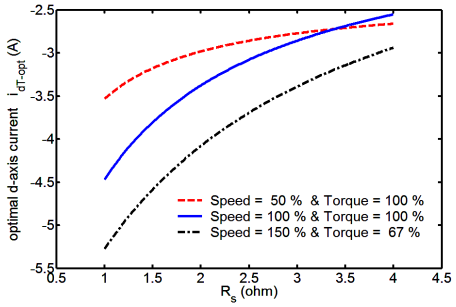

Fig. (4): Influence of R_s variations on optimal i_{dT}

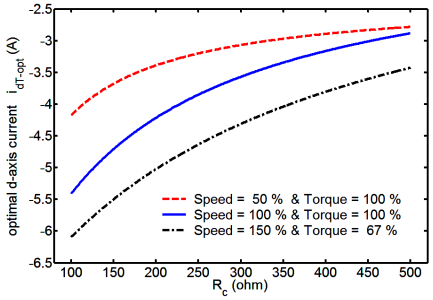

Fig. (5): Influence of R_c variations on optimal i_{dT}

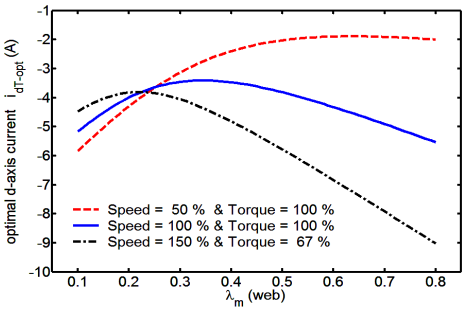

Fig. (6): Influence of λ_m variations on optimal i_{dT}

It can be seen that except near the nominal operating conditions, gradients of the curves are significant, emphasizing again the necessity for machine parameter estimation in model based EOCs [9,10].

Finally a systematic sensitivity analysis is carried out to better comprehend the influence of parameter variations on the optimal i_{dT}. The sensitivities of optimal i_{dT} to R_s, R_c and λ_m can be found by partial differentiation of (10) with respect to these parameters and rearranging the results to obtain:

$$S_{R_s} = \frac{\partial i_{dT}}{\partial R_s} = -\frac{1}{K}\left(\frac{\partial a_4}{\partial R_s} i_{dT}^4 + \frac{\partial a_3}{\partial R_s} i_{dT}^3 + \frac{\partial a_2}{\partial R_s} i_{dT}^2\right) + \frac{\partial a_1}{\partial R_s} i_{dT} + \frac{\partial a_0}{\partial R_s} \qquad (11)$$

In particular, the on-line estimation of equivalent iron loss resistance has not been presented in the literature at all to the best of authors' knowledge. The estimation of other parameters of IPM synchronous motors has been widely proposed in the literature for motor control systems other than EOCs. In particular extended Kalman filter (EKF) is used [11-12]. The main difficulty with EKF is the selection of covariance matrix of noise and the algorithm initial values. Also, model reference adaptive system (MARS) is used for the estimation of the motor parameters [13-14]. This is an effective estimation method. However, it strongly depends on the machine model and runs into difficulty in selecting the parameters of adaptation law. Extended Luenberger observer (ELO) can also be used if the gain matrix is selected appropriately [15].

In this paper, the adverse effect of motor parameter variations on minimum loss operation of IPM synchronous motors is rather comprehensively analyzed first. Then an accurate, yet simple observer is designed for estimating the copper loss and iron loss parameters and PM flux linkage of the motors. Theoretical analysis confirms that the stability and convergence of the proposed observer is guaranteed. The observer is next incorporated into a proposed nonlinear feedback linearization IPM synchronous motor control system that ensures high performance and optimized efficiency operation. Finally, extensive simulation results are presented to show efficient, high performance and robust motor drive operation under the proposed control system.

II. Machine Model

Under certain assumptions a widely used model for IPM synchronous motors including copper and iron losses in a synchronously rotating reference frame is presented in Fig. 1 [3,9].

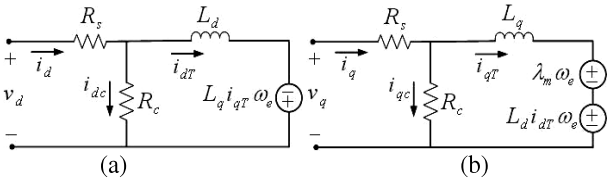

Fig. (1): Equivalent circuits for IPMSM considering the iron losses.
(a) d axis. (b) q axis.

The motor d-and q-axis voltages and torque are given as follows:

$$v_d = R_s i_{dT} + \left(1+\frac{R_s}{R_c}\right)\left(L_d p i_{dT} - \omega_e L_q i_{qT}\right) \quad (1)$$

$$v_q = R_s i_{qT} + \left(1+\frac{R_s}{R_c}\right)\left(L_q p i_{qT} + \omega_e\left(\lambda_m + L_d i_{dT}\right)\right) \quad (2)$$

$$T_e = \frac{3P}{2}\left(\lambda_m + \left(L_d - L_q\right) i_{dT}\right) i_{qT} \quad (3)$$

In steady state condition, voltage equations reduce to:

$$v_d = R_s i_{dT} - \left(1+\frac{R_s}{R_c}\right) L_q \omega_e i_{qT} \quad (4)$$

$$v_q = R_s i_{qT} + \left(1+\frac{R_s}{R_c}\right)\left(\lambda_m + L_d i_{dT}\right) \omega_e \quad (5)$$

The copper and iron losses of the IPM synchronous motors can also be calculated from Fig. 1 as follows:

$$P_c = \frac{3}{2} R_s \left(i_d^2 + i_q^2\right),\ P_i = \frac{3}{2} R_c \left(i_{dc}^2 + i_{qc}^2\right) \quad (6)$$

where i_{dc} and i_{qc} are the current components responsible for iron losses, which can be calculated as:

$$i_{dc} = i_d - i_{dT} = \frac{v_d - R_s i_d}{R_c}, i_{qc} = i_q - i_{qT} = \frac{v_q - R_s i_q}{R_c} \quad (7)$$

Thus, using (4) - (7), the total electrical power losses of the IPM synchronous motors can be expressed as:

$$P_L = P_c + P_i = \frac{3}{2} R_s \left(i_{dT}^2 + i_{qT}^2\right) + 3\frac{(R_s + R_c)}{R_c^2} L_d \lambda_m \omega_e^2 i_{dT}$$
$$+ \frac{3}{2}\frac{\omega_e^2}{R_c^2}\left(R_s + R_c\right)\left(\lambda_m^2 + \left(L_d^2 i_{dT}^2 + L_q^2 i_{qT}^2\right)\right) \quad (8)$$
$$+ 3\frac{R_s}{R_c}\left(\lambda_m + \left(L_d - L_q\right) i_{dT}\right) \omega_e i_{qT}$$

III. Sensitivity analysis of minimum loss

In general the motor parameters vary over wide ranges depending on the operating conditions and the ambient temperature. In many IPM synchronous motors these variations are dominant due to the motor construction [16]. In particular, R_s changes due to a temperature rise; R_c varies with the motor speed, and also due to the saturation in the iron bridges between rotor magnets; and λ_m varies due to aging, temperature effect and partial demagnetization. These variations affect the motor characteristics and performance including the minimum loss operation [10]. In this section the effects are studied first. Then a detailed sensitivity analysis is carried out to better quantify the variation effects.

Combining (8) and (3) and eliminating i_{qT}, yields:

$$P_L = \frac{3}{2} R_s i_{dT}^2 + \frac{3(R_s + R_c)}{R_c^2} L_d \lambda_m \omega_e^2 i_{dT} + \frac{2}{P}\frac{R_s}{R_c}\omega_e T_e$$
$$+ \frac{2T_e^2}{3P^2(\lambda_m + (L_d - L_q) i_{dT})^2}\left(\frac{(R_s + R_c)}{R_c^2} L_q^2 \omega_e^2 + R_s\right) \quad (9)$$
$$+ \frac{3(R_s + R_c)}{2R_c^2}\left(\lambda_m^2 + L_d^2 i_{dT}^2\right)\omega_e^2$$

Plotting (9) versus i_{dT} as in Fig. 2, for a motor with specifications as presented in Appendix I, confirms that the motor electrical loss reaches a minimum at point A if i_{dT} is adjusted by an EOC to an optimal value.

Also it shows that the individual variations of R_s, R_c and λ_m near the nominal speed and torque operation shift the minimum value of P_L to points B, C and D respectively if a corresponding optimal value of i_{dT} is applied to the machine in each case [3]. However, in a model based EOC system, without a means for inclusion of parameter variations into the control system, a fixed value of i_{dT} corresponding to point A is found out from the machine model with constant parameters and applied to the motor, as an assumed optimal i_{dT} command signal.

Efficiency Optimization Control of IPM Synchronous Motor Drives with Online Parameter Estimation

Sadegh Vaez-Zadeh[(1)] - Mehran Zamanifar[(2)]
(1) Professor - Department of Electrical Engineering, Tehran University,Tehran, Iran
(2) Ph.D Candidate - Department of Electrical Engineering, Isfahan University of Technology, Isfahan, Iran

Recive: Autumn 2009 Accept: Spring 2010

Abstract: This paper describes an efficiency optimization control method for high performance interior permanent magnet synchronous motor drives with online estimation of motor parameters. The control system is based on an input-output feedback linearization method which provides high performance control and simultaneously ensures the minimization of the motor losses. The controllable electrical loss can be minimized by the optimal control of the armature current vector. It is shown that parameter variations except at near the nominal conditions have undesirable effect on the controller performance. Therefore, a parameter estimation method based on the second method of Lyapunov is presented which guarantees the stability and convergence of the estimation. The extensive simulation results show the feasibility of the proposed controller and observer and their desirable performances.

Index Terms: Synchronous motors, permanent magnet motors, efficiency optimization control, parameter estimation, input-output feedback linearization.

I. Introduction

Energy saving solutions of electric motor drives have received considerable attention during the last three decades due to scarcity of primary energy sources, increasing electric energy cost and air pollution. These solutions include increased use of high efficiency motors and efficiency optimization control of motor drives. Permanent magnet synchronous motors benefit from the highest efficiency among electric motors [1-2]. Interior permanent magnet (IPM) synchronous motors particularly enjoy potential high efficiency plus other advantages like high power density, mechanical robustness, enhanced flux weakening and high speed capabilities. However, a high efficiency in these motors can only be realized under appropriate control strategies. Thus much effort has been directed towards the efficiency optimization control (EOC) of IPM synchronous motors by minimizing machine losses [3-7]. The existing EOC methods are divided into two main categories. One category consists of on-line or searching methods in which the machine model is not used in loss minimization. However, care must be taken to overcome torque ripples and long search time associated with these methods [4,8]. The other category includes the model-based EOC methods which are very fast and do not produce torque ripples. Therefore, they have been the most widely used methods so far.

Regardless of the works which have considered the minimization of copper loss only; there exist many papers on model based EOC of IPM synchronous motors which take into account both the copper loss and the iron loss in the loss minimization by varying degree of accuracy. For instance, the iron loss has been considered by approximate relationships in which a true maximum efficiency may not be achieved [6]. In other works the iron loss is modeled more accurately [3,5,7]. However, in these works like other works mentioned above, the motor parameter variations have not been taken into account [3,5,6]. These variations may occur over a wide range and due to different factors. The stator resistance may vary due to skin effects, temperature variations, etc. Core loss also varies due to the variations of motor flux and speed and become an important issue at high speeds [7]. Also permanent magnet (PM) flux may vary due to temperature variations, excessive flux weakening, etc. Nevertheless, it has been shown, by a simulation study that the parameter variations have marginal effects on EOC of IPM synchronous motor drives; thus an efficiency optimization control with nominal parameters has been proposed [3]. However, the study has only been carried out at the nominal motor operating point. It is shown that the parameter variations my lead to a suboptimal or even reduced efficiency at non-nominal operating points [9-10]. Therefore, it is vital to include parameter variations into account in model based EOC of variable speed motor drives. One solution is to model motor parameters as functions of motor operating point by measurement of parameters over a range of possible operating points [7]. This method is machine dependent and needs many measurements for each motor.

An on-line motor parameter estimation is another means for taking parameter variations into account in model based EOCs.

Such parameter estimation has not been incorporated into EOC of IPM synchronous motor drives so far.